

# Use of expanded copper mesh grid for negative electrodes of sealed lead storage batteries

M. Lushina, Yu Kamenev\*, V. Leonov, E. Ostapenko

Scientific Research Center JSC "Electrotyaga", 50-a Kalinin Str., St. Petersburg 198095, Russia

Received 24 June 2004; received in revised form 25 January 2005; accepted 31 January 2005

Available online 16 March 2005

## Abstract

Effect of electrolysis conditions on properties of electroplating of lead and its alloys is studied. It is shown that two-layer electroplating (the first layer of lead–tin–zinc alloy and the second layer of lead) using nitrilotriacetate-electrolyte (NTA-electrolyte) applied to expanded copper mesh grid (ECMG) of negative electrodes ensures reliable copper protection against the contact with storage battery electrolyte and makes it possible to use ECMG in sealed storage batteries.

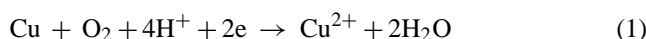
© 2005 Elsevier B.V. All rights reserved.

**Keywords:** VRLA; Expanded copper mesh grid; Layer electroplating

## 1. Introduction

Negative electrodes with lead plated expanded copper mesh grid (ECMG) [1–3] are used in lead acid industrial-purpose storage batteries with the aim to improve specific mass characteristics and to facilitate current distribution. ECMG are used due to reduced specific gravity, as compared to the lead, high-electric conductivity, as well as sufficient strength and good machinability. But it is impossible to use copper without its protection against contact with electrolyte, since copper is able to considerably increase the rate of hydrogen-evolution from a storage battery. Nowadays, lead electroplating 20–30  $\mu\text{m}$  thick is used to protect copper sheets. But such plating cannot ensure reliable protection of copper sheets at long-term service life (10 years and more). In the negative electrode operation process, the plating lead can participate in the current generating process and this can result in increased porosity of the protection layer.

In this case, copper under such plating will be dissolved according to the reaction:



\* Corresponding author. Tel.: +7 812 316 96 43; fax: +7 812 186 97 55.  
E-mail address: [lushina@mail.wplus.net](mailto:lushina@mail.wplus.net) (Y. Kamenev).

and then can be contact deposited on the surface of the negative active mass (NAM). The minimum theoretic concentration of copper in the solution,  $a_{\text{Cu}}$  at which its contact deposition begins, can be calculated from the relationship:

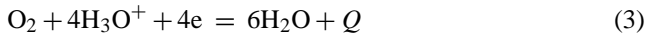
$$a_{\text{Cu}^{2+}} = \exp\left[\frac{4F(E_{\text{Pb}} - E_{\text{Cu}}^0)}{RT}\right] = 10^{-23} \text{ mole l}^{-1} \quad (2)$$

where  $F$  is the Faraday constant,  $R$  the gas constant,  $T$  the temperature, and  $E_{\text{Pb}}$  and  $E_{\text{Cu}}^0$  are the potential of negative electrode and copper equilibrium potential, respectively. In practice, an appreciably increased gas-evolution has been noted at copper concentration at a degree of  $4.8 \times 10^{-4} \text{ mole l}^{-1}$  [4].

In sealed lead storage batteries, ECMG are not used nowadays and this is stemming from the fact that no high-efficient protective plating are available and that permissible copper concentrations in electrolyte are extremely low.

Yet, use of copper sheets in industrial sealed storage batteries is deemed as necessary. Firstly, sealing of a lead storage battery reduces its specific power characteristics by 15–20% on the average and refusal from using ECMG will result in ever decreased such characteristics particularly under conditions of intensive discharge. Secondly, in sealed storage

batteries, unlike of the usual batteries, there appears a new powerful source of heat associated with oxygen reduction on negative electrodes:



This heat source appears due to the fact that unlike closed systems, in which evolved gas (oxygen and hydrogen) leaves the storage battery, unlike opened systems oxygen must be reduced on negative electrode according to reaction (3).

In addition, used in sealed lead acid storage batteries (VRLA) is a limited amount of electrolyte, which to a great degree determines the storage battery heat capacity and in combination with a relatively low-heat capacity of lead storage battery tank walls also facilitates its heating.

And finally, owing to design peculiarities of the VRLA, it is not possible to use such effective method of electrolyte cooling as its stirring with simultaneous heat release to refrigerators.

It is clear that ensuring heat balance becomes more difficult as storage battery nominal capacity increases, since heat release is proportional to active mass amount, i.e., conventionally to storage battery dimension in the third power, and heat removal is proportional to storage battery surface, i.e., to storage battery dimension in the second power.

Considering a relative low-heat conductivity of tank materials and lack of electrolyte stirring, heat from the electrode unit of sealed storage batteries is released, mainly along the electrodes to cooled terminals. Use of ECMG will make it possible to increase the rate of heat transfer due to considerable increase of heat conductivity of negative electrode (heat conductivity of copper and lead are equal to 326 and 29.9 kcal m<sup>-1</sup> h<sup>-1</sup> deg<sup>-1</sup>). Efficiency of using copper in the negative electrodes is determined by the fact that it is the heat releasing reaction of oxygen reduction that is localized on a negative electrode. And finally, surplus NAM [5] is required for operation of a sealed storage battery in the emergency-backup mode. This can be ensured by using ECMG that make it possible to have a large volume of active mass in an electrode. Use of ECMG will make it possible to considerably increase strength of negative electrodes and their adaptability to manufacture.

Thus, development of high-efficient protective plating ensuring reliable insulation of copper grids from electrolyte during a long service life of storage batteries is an important stage in industrial sealed storage battery production.

Plating protective properties can be improved by using an intermediate layer of corrosion-resistant alloy located between the copper grid and the lead plating.

Electroplating with tin 5 μm thick is proposed as such additional layer in paper [6]. But tin electroplating has a coarse-crystalline structure and is porous at a layer thickness of at least 25 μm. This results in creation of contact pair Cu–Sn and accelerates the tin dissolution process due to its contact with copper. It is known that tin has a high-overvoltage of hydrogen-evolution and its corrosion takes place with oxygen

depolarization. Under these conditions, tin corrosion,  $V_{\text{corr}}$  can be evaluated from the relationship:

$$M_{\text{Sn}} = K j_{\text{Sn}} S \tau; \quad j_{\text{Sn}} = j_{\text{O}_2}; \quad j_{\text{O}_2} = \frac{4FD_{\text{O}_2}C_{\text{O}_2}}{\delta};$$

$$V_{\text{corr}} = \frac{M_{\text{Sn}}}{S\tau} = \frac{4KF D_{\text{O}_2} C_{\text{O}_2}}{\delta} \quad (4)$$

where  $\tau$  is the time;  $M_{\text{Sn}}$  the mass of dissolved tin during the time  $\tau$ ;  $S$  the electrode surface area;  $K$  the electrochemical equivalent;  $j_{\text{Sn}}$  and  $j_{\text{O}_2}$  the density of tin dissolution current and density of oxygen reduction current, respectively;  $D_{\text{O}_2}$  and  $C_{\text{O}_2}$  the diffusion factor and dissolved oxygen concentration, respectively; and  $\delta$  is the diffusion layer thickness. Substituting in (4) the known values of  $K$ ,  $F$ ,  $D_{\text{O}_2}$ ,  $C_{\text{O}_2}$ , and  $\delta$ , one can evaluate the rate of tin corrosion as 13.3 g m<sup>-2</sup> h<sup>-1</sup>. The value of tin corrosion rate within a range of 6.3–25 g m<sup>-2</sup> h<sup>-1</sup> depending on dissolved oxygen content is given in paper [7]. Under real conditions of a negative electrode operation, tin corrosion will be less than the above mentioned value, since the tin layer is coated with the lead layer, which has sulphate film at a boundary with electrolyte. The latter is a barrier for oxygen transfer [8] it reduces the value of  $C_{\text{O}_2}$  in pores of the lead layer at the boundary with tin and according to (4) reduces the rate of its corrosion. But due to low-overvoltage of hydrogen-evolution on copper and high-mobility of protons at contact of tin with copper, a reaction of hydrogen-reduction is developed, which will increase the rate of tin layer dissolution. Thus, tin plating cannot guarantee a reliable protection of copper sheets.

To reduce porosity of tin plating, Kamenev et al. [9] propose to melt it. But processes, which considerably affect the protective characteristics of the tin plating, are developed at the boundary of tin-copper at melting. In paper [9], it is shown that at tin melting easily melted η-phase is created in the first moment (Cu<sub>6</sub>Sn<sub>5</sub>). The electronic microscopic analysis has shown that the tin layer area adjoining to copper has inclusions of acicular crystals of the intermetallides. At increased melting temperature and time intermetallide layer, thickness significantly increases. The intermetallides Cu<sub>6</sub>Sn<sub>5</sub> serve as a cathode in relation to tin [7], and hence their penetration to the tin layer external surface will cause appearance of contact pair Sn|Cu<sub>6</sub>Sn<sub>5</sub>, which expedites tin dissolution. Thus, increased time of tin layer melting can be the cause of its protective characteristic deterioration, and therefore its correct selection is one of the determining parameters of two-layer plating applying process.

It is known that alloy plating, as a rule, possesses higher protective properties as compared to pure metal plating [10]. Thus, alloys Pb–(4–10) wt.% Sn have a relatively high-corrosion resistance [10]. But according to the data of papers [11,12], they sharply lose their corrosion resistance after a certain time of their keeping in a corrosive medium. Introduction of zinc into the alloy Pb–Sn facilitates a sharp improvement of its corrosion resistance [10]. Lushina and Kolikova [13] have shown that the alloy Pb–(6.0–8.0) wt.%

Sn-(0.5–1.0) wt.% Zn, which is applied from boron fluoride-electrolyte (BFE) by electroplating methods on a copper surface, has high-protective characteristics. Corrosion rate of such alloy is  $0.03 \text{ mg cm}^{-2} \text{ year}^{-1}$ , and this rate is considerably lower than corrosion rate of tin ( $38.7 \text{ mg cm}^{-2} \text{ year}^{-1}$ ) and lead ( $30.7 \text{ mg cm}^{-2} \text{ year}^{-1}$ ) under similar conditions. Based on the obtained results in paper [13], it is proposed to protect ECMG of lead storage battery negative electrode with the help of a two-layer plating, i.e., a layer of the alloy Pb-(6.0–8.0) wt.% Sn-(0.5–1.0) wt.% Zn and a layer of the lead plating. It has been shown that plating with the layer of Pb-(6.0–8.0) wt.% Sn-(0.5–1.0) wt.% Zn makes it possible to ensure service life of negative ECMG up to 5–6 years.

The main disadvantage of the plating proposed by the authors [13] is non-uniformity of its thickness over the surface of the expanded copper sheet due to low-dissipating ability of the BFE as well as due to the tendency to form lead dendrite deposits in the places with increased current density. In addition, the BFE have high-corrosive properties and use of this electrolyte brings ecological problems at production.

It is possible to considerably improve characteristics of plating with the alloy Pb–Sn–Zn and lead by using electrolyte with high-dissipating capacity, which ensures creation of dense fine-crystalline deposits.

The target of this paper is studying the possibility to obtain two-layer plating (a layer of alloy Pb–Sn–Zn and a layer of lead) with protective characteristics improved due to use of fresh electrolyte.

Analysis of patent and scientific literature has made it possible to assume that nitrilotriacetate-electrolyte (NTA-electrolyte) is perspective electrolyte for depositing lead and its alloys. This electrolyte is easily prepared, it is stable with time and not toxic. The main component of this electrolyte is nitrilotriacetic acid ( $\text{N} \equiv (\text{CH}_2\text{COOH})_3$ ).

A sufficiently great attention is paid to the problem of creating lead and tin complexes with the nitrilotriacetic acid both in foreign and home literature. In papers [14,15], it is shown that at nitrilotriacetate ions concentration of  $3 \times 10^{-3}$  to  $5 \times 10^{-2} \text{ M}$ , within a range of pH 1.7–3.3, complexes  $\text{PbNTA}^-$  and  $\text{PbHNTA}$  are created; within a range of pH 3.4–7.4, complex  $\text{PbNTA}^-$  is formed; within a range of pH 7.5–10.4, complexes  $\text{PbNTA}^-$  and  $\text{Pb}(\text{NTA})_2^{4-}$  are created; and within a range of pH 10.5–12.9, complexes  $\text{PbNTA}^-$ ,  $\text{Pb}(\text{NTA})_2^{4-}$ ,  $\text{PbOHNTA}^{2-}$ , and  $\text{Pb}(\text{OH})_3^-$  are formed.

In paper [16], lead(II) ion electroreduction from the NTA-electrolyte is studied and a possibility of obtaining lead plating with fine-crystalline structure from it is shown. According to the data of paper [17], it is possible to obtain tin plating from the NTA-electrolyte. Surfactant admixtures being added to this electrolyte, light-colour fine-crystalline tin plating with improved protective characteristics is formed. With tin, the NTA forms complexes of  $\text{SnHNTA}$ ,  $\text{SnNTA}^-$ , and  $\text{Sn}(\text{NTA})_2^{4-}$  types depending on the pH [17]. Patterns of mutual discharge of lead(II) and tin(II) ions in the NTA-electrolyte have been studied by authors [18] and the pos-

sibility Pb–Sn alloy plating deposition from this electrode is shown.

Taking into consideration the fact that in the NTA-electrolyte ions of lead(II) and tin(II) forms complexes of different kinds (dependence of structure of  $\text{Pb}(\text{II})$ -NTA and  $\text{Sn}(\text{II})$ -NTA complexes on pH are presented in [14,15,17]), it is possible to obtain plating of stable quality only at strict observation of the electrolysis. Therefore, the problem of studying effect of electrodeposition parameters on plating properties is rather important. Optimization of these parameters will make it possible to obtain plating, which is able to protect the copper sheet of storage battery negative electrodes during a long-term service life, as well as to use copper grids in sealed storage batteries.

## 2. Experiment results and their discussion

### 2.1. Lead plating

To determine the effect of various technological factors on the quality of the obtained plating lead electrodeposition has been carried out at changing the following parameters:

- rate of electrolyte stirring;
- electrolyte temperature ( $20\text{--}70 \text{ }^\circ\text{C}$ );
- cathode current density ( $10\text{--}260 \text{ A m}^{-2}$ );
- lead(II) ion concentration ( $0.3\text{--}0.5 \text{ mole l}^{-1}$ );
- nitrilotriacetate ion concentration ( $0.6\text{--}0.9 \text{ mole l}^{-1}$ );
- solution pH 3–8;
- surfactant admixture concentration ( $0\text{--}7 \text{ g l}^{-1}$ ).

To finalize electrolyte composition, electrolyses with changed concentration of each solution component at other equal conditions have been carried out. Polyethylene glycol (PEG) has been used as a surfactant admixture (SA) for leading the NTA-electrolyte.

Since cathode polarization value reduces with the increase of lead(II) ion concentration coarsening of crystals takes place. Thus, with lead(II) ion concentration below  $0.4 \text{ mole l}^{-1}$  fine-crystalline plating is formed (Fig. 1a). If such concentration is above  $0.4 \text{ mole l}^{-1}$ , plating quality becomes worse because of formation on the entire cathode surface of loose deposits like dendrites (Fig. 1b).

Effect of the SA on plating structure has been studied within a wide concentrations of the admixture. It has been stated that the SA optimal concentration is  $5 \text{ g l}^{-1}$ ; the concentration above this value does not exert any considerable effect on the plating quality. Deposits from the electrolyte without the SA have been obtained as reference specimens (Fig. 1c): the specimens had poorly plated surface; lead large crystals have been shed from the copper sheet.

Studies of electrolyses mode effect on the plating quality have shown that the process of leading from the NTA-electrolyte shall be conducted only with electrolyte stirring, since the kinetics of lead depositing in this electrolyte depends on hydro-dynamic conditions. Polarization measure-

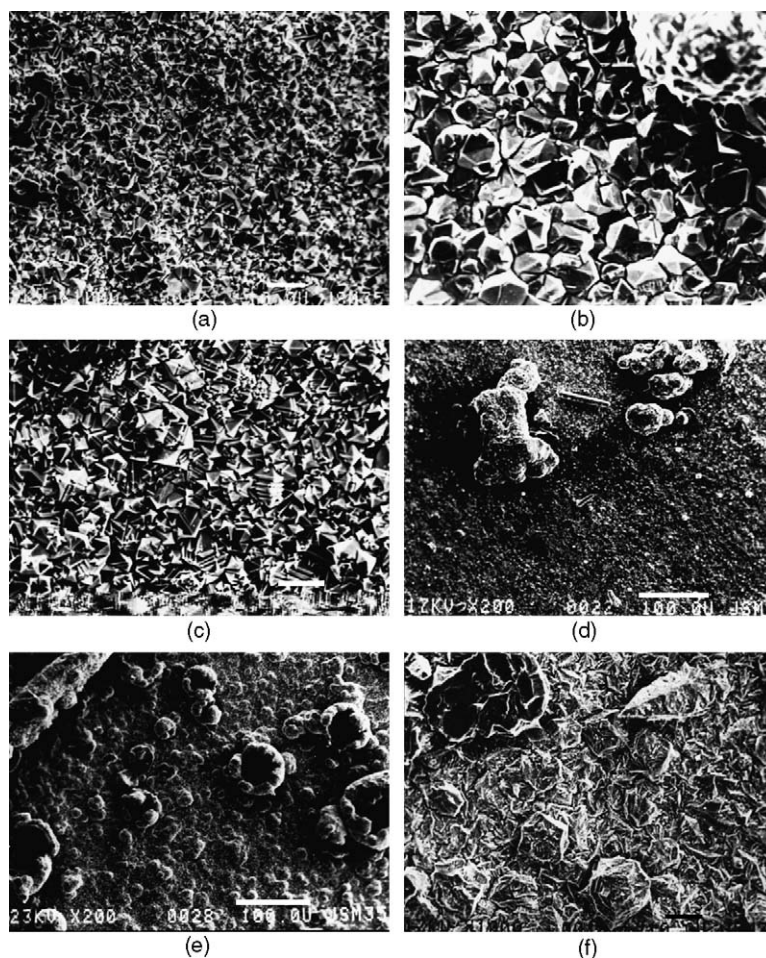


Fig. 1. Effect of various technological factors on microstructure of lead electroplating obtained from nitrotriacetate-electrolyte. (a) lead(II) ion concentration is below  $0.4 \text{ mole l}^{-1}$ ; (b) lead(II) ion concentration is above  $0.4 \text{ mole l}^{-1}$ ; (c) no SA; (d) without stirring; (e) current density exceeds limiting diffusion current value; and (f) electrolyte temperature is  $60^\circ\text{C}$ . Magnification:  $\times 1000$  in (a–c and f);  $\times 200$  in (d and e).

ments have shown that discharge of the complex  $\text{PbNTA}^-$  results in evolution of the  $\text{NTA}^{3-}$  ions. As a result, possibility of forming complexes with a large number of ligands (for example,  $\text{Pb}(\text{NTA})_2^{4-}$ ) in the near-electrode layer increases on one side and on the other side, possibility of near-cathode layer alkalization and formation of mixed hydroxo-complexes also increases. Under these conditions, rate of lead depositing reduces, since discharge of stronger complex takes place at more negative potentials. Thus, without stirring plating quality has become worse (Fig. 1d): dendrites have been formed on the surface, near-cathode space has become dimmed (due to  $\text{PbOHNTA}^{2-}$  formation), hydrogen-evolution has taken place. Electrolyte stirring results in accelerated tapping of surplus ligands from the solution layer adjoining the cathode surface, and thus the effect of lead ions discharge retarding becomes less under such conditions. Therefore, later on all electrolyses have been conducted only with stirring.

Current density value has a great influence on the structure of obtained lead plating deposits. Increased current density has facilitated formation of fine-grained lead deposits on the cathode, and this is explained by increased amount of ac-

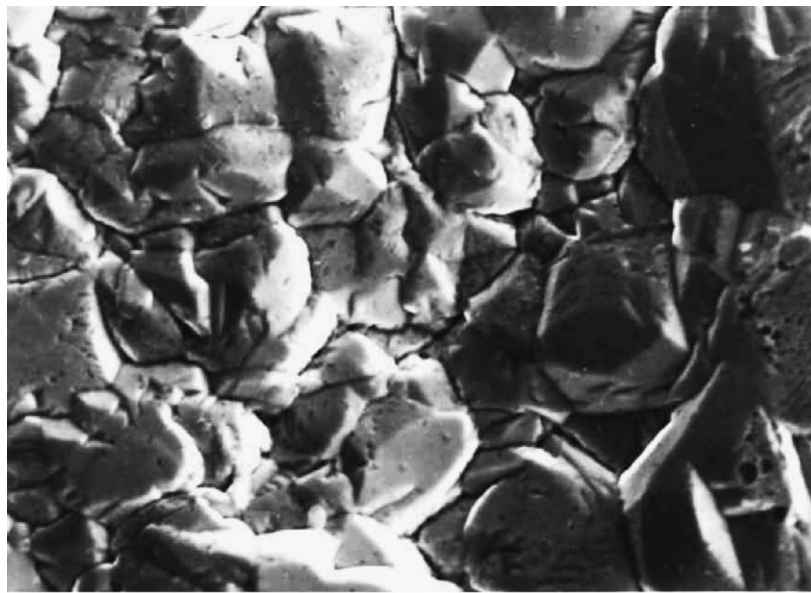
tive and simultaneously growing, places of cathode surfaces. But at very high-current densities (near to the limiting value of diffusion current) formation of loose deposits like dendrites took place (Fig. 1e). Dendrite formation is explained by preferential growth of crystals on separate sections, on which due to not uniform current distribution, such current density is set, which exceeds the permissible limit for this electrolyte.

Study of temperature effect on the lead electrodeposition and characteristics of obtained plating has shown that increased temperature results, on one side in accelerated release of surplus ligands from the solution layer adjoining the cathode surface, and hence in reduction of effects of lead ions discharge retarding under these conditions and on the other side, it results in depositing more coarse-crystalline deposits. Thus, at a temperature exceeding  $40^\circ\text{C}$  plating sediments have had coarse-crystalline structure and this is explained by a partial desorption of PEG from the electrode surface under the action of high-temperature. When temperature reaches  $60^\circ\text{C}$ , the electrolyte loses its transparency; a film and traces of a compound of organic nature appear on the solution surface. It is clear that at the specified temperature, PEG decom-

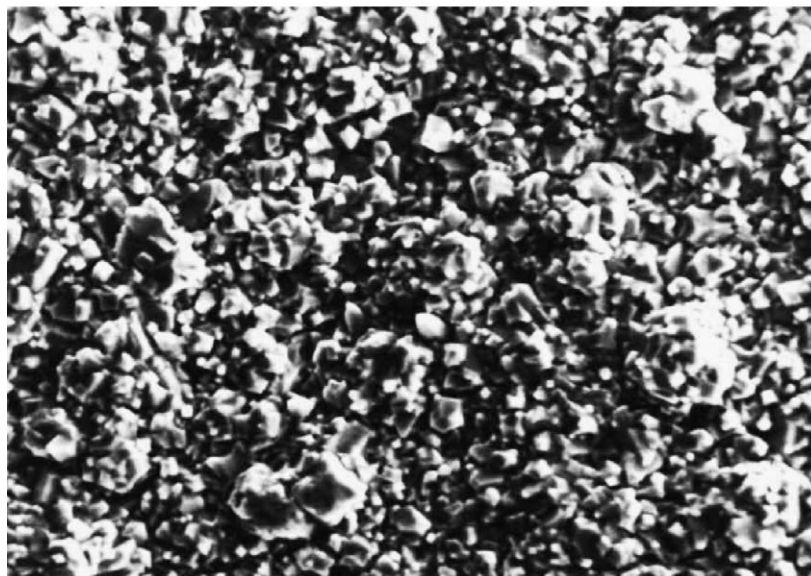
position takes place. In this case, plating of unsatisfactory quality is obtained: it is of dark colour with significant grow of dendrites as “fringe” in all directions. At a temperature above 60 °C, the microstructure character has significantly changed: formation of flaky deposits took place (Fig. 1f).

Based on the obtained results NTA-electrolyte optimal composition for leading and electrolysis mode ensuring high-quality plating have been determined. Fig. 2 shows the lead plating obtained from the NTA-electrolyte of the selected composition. For the purpose of comparison of protective characteristics of lead plating obtained from the NTA-electrolyte, and lead plating obtained from the BFE-electrolyte, microstructure and porosity have been studied. Microstructure study of the lead plating obtained from the

BFE-electrolyte has shown that the surface (a fragment of the surface is shown in Fig. 2a) represents a disordered alternation of large and small blocks of irregular shape: No predominant directed growth of crystals is observed. The crystals have a linear size of about 10  $\mu\text{m}$ . Lead plating obtained from the NTA-electrolyte (Fig. 2b) by its outward appearance is more uniform and fine-crystalline (crystal liner size is 1–2  $\mu\text{m}$ ), which causes its better physical and chemical properties as compared to the plating deposited from the BFE-electrolyte. Thus, light-colour, half-brilliant, strongly adhered to the copper sheet plating with increased corrosion resistance without pores at a thickness of even 5  $\mu\text{m}$  is formed from the NTA-electrolyte. Obtaining of non-porous lead plating from the BFE-electrolyte is possible only at thickness above 20  $\mu\text{m}$ .



(a)



(b)

Fig. 2. Microstructure of lead electric plating obtained from hydrogen boron fluoride-electrolyte (a) and nitrilotriacetate-electrolyte (b). Magnification:  $\times 1000$ .

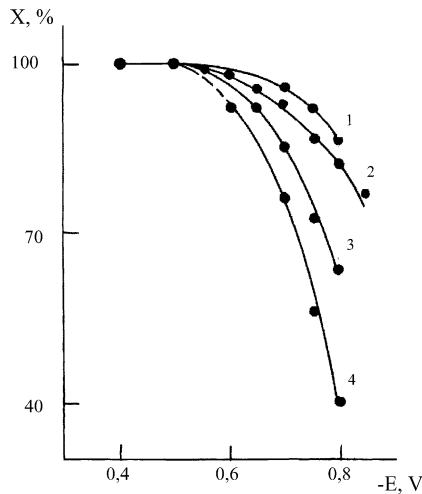


Fig. 3. Dependence of lead content  $X$  (mass%) in Pb–Sn alloy on cathode potential in nitrilotriacetate solution at different ratio of Pb(II) and Sn(II) ions concentration ( $C_{Pb(II)}:C_{Sn(II)}$ ): (1) 2:1; (2) 1:1; (3) 1:2; (4) 1:4.  $E$ , potential (V) (potential vs. standard hydrogen el.).

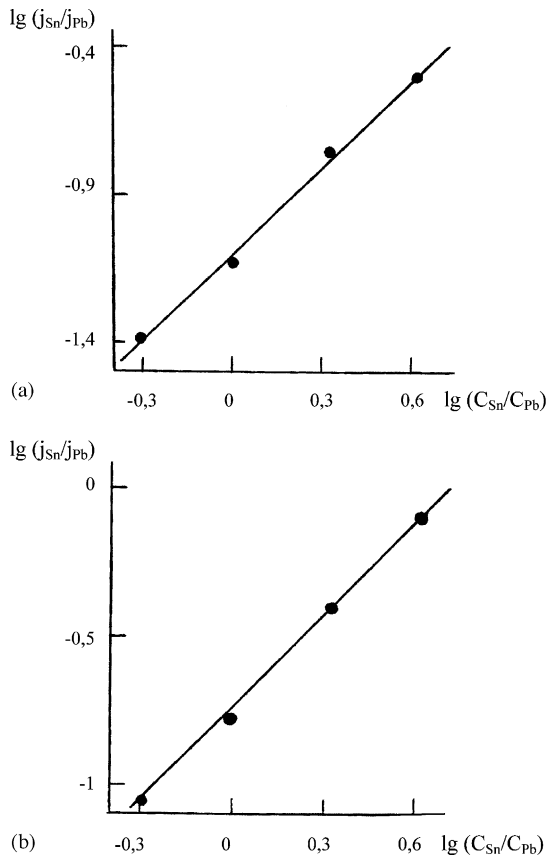


Fig. 4. Dependence of Pb–Sn alloy composition on composition of nitrilotriacetate-electrolyte for deposition of this alloy. Deposition potentials (V): (a)  $-0.7$ ; (b)  $-0.75$  (potential vs. standard hydrogen el.). Current density,  $j$  ( $A\ m^{-2}$ ) and concentration of components,  $C$  ( $mole\ l^{-1}$ ).

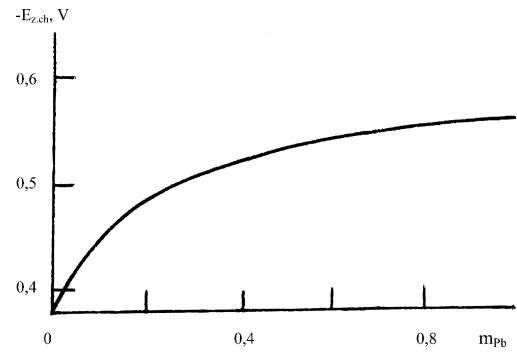


Fig. 5. Dependence of zero charge potential,  $E_{z.ch.}$  (V) of Pb–Sn alloy on lead mole fragment,  $m_{Pb}$ .

### 2.2. Pb–Sn–Zn alloy plating

Since any change in electrolyte composition causes, as a rule, changes not only of the obtained plating quality, but alloy structure and composition, then it is difficult to predict possibility of alloy electrodepositing from the preset electrolyte and its composition. These data can be obtained only by experimental way. But there are some cases when alloy composition can be determined on the basis of general kinetic laws:

- (1) when electrically positive metal is obtained at limiting diffusion current and electrically negative one is obtained with retarded discharge stage;
- (2) when both metals are obtained with limiting diffusion current.

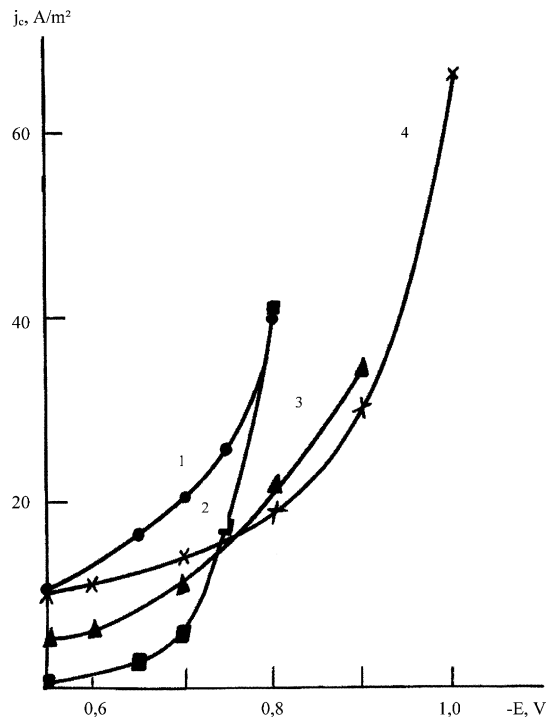


Fig. 6. Partial polarization curves of lead (1) and tin (2) evolution to alloy and to pure phase (4 and 3), respectively, in nitrilotriacetate-electrolytes.

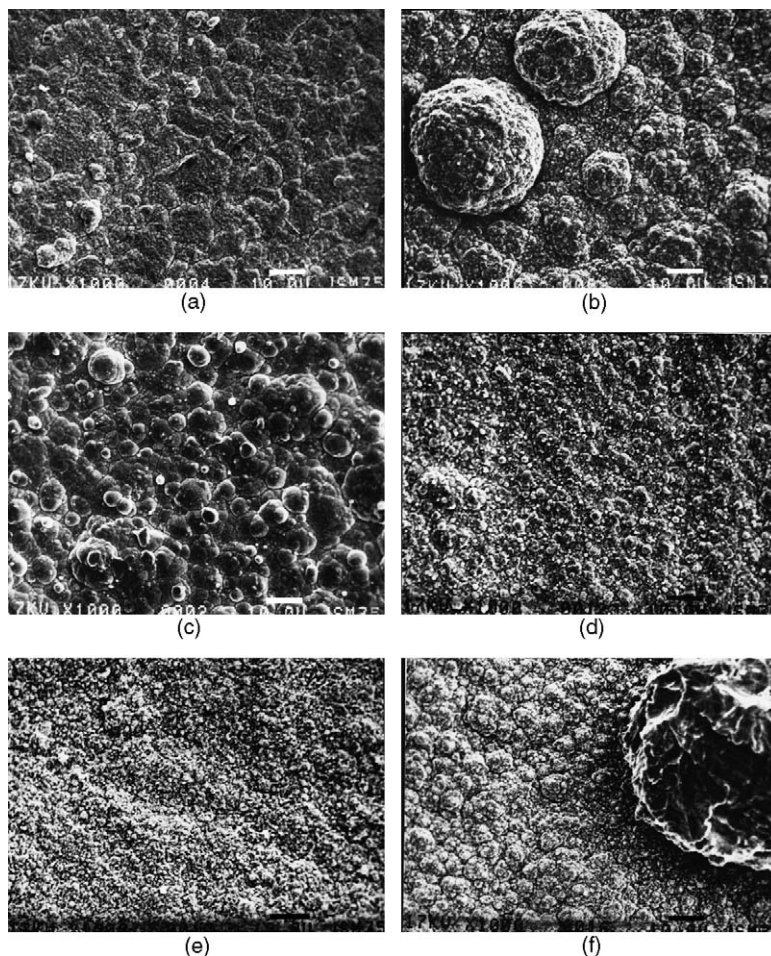


Fig. 7. Microstructure of Pb–6 wt.% Sn alloy plating (a–c) and Pb–6 wt.% Sn–0.75 wt.% Zn alloy plating (d–f) obtained from nitrilotriacetate-electrolyte. Current density ( $A\ m^{-2}$ ): (a and e) 28; (c and d) 56; (b and f) 278. Magnification:  $\times 1000$ .

Study of laws of separate and combined discharge of lead(II), tin(II), and zinc(II) ions in the NTA-electrolyte by the polarization method has shown that tin ion discharge takes place in the background of lead ion discharge limiting current. Therefore, tin in the alloy can be detected only beginning with a potential certain value and its content will rise as the cathode polarization increases. As shown in Fig. 3, the mentioned above considerations can be observed in experience

and the higher tin content in the electrolyte, the alloy with higher tin content deposited on the cathode.

One of the main requirements of the theory of ion-combined discharge is strict correspondence between partial currents of discharge of ions—components of the alloy,  $j$  and concentrations of ions under discharge in the electrolyte [19]:

$$\log \frac{j_1}{j_2} = \text{const} + \log \frac{C_{01}}{C_{02}} \quad (5)$$

Table 1

$-E$ (V)	Alloy composition		$j_{\Sigma}$ ( $mA\ cm^{-2}$ )	$j_{Pb}$ ( $mA\ cm^{-2}$ )	$j_{Sn}$ ( $mA\ cm^{-2}$ )	$j_{Pb} + j_{Sn}$ ( $mA\ cm^{-2}$ )	$f_{Pb}$	$f_{Sn}$	$j'_{Pb}$ ( $mA\ cm^{-2}$ )	$j'_{Sn}$ ( $mA\ cm^{-2}$ )
	Pb (wt.%)	Sn (wt.%)								
0.55	99	1	1.3	1.15	0.02	1.17	0.98	0.02	1.2	1.3
0.65	92	8	2.1	1.7	0.3	2.0	0.88	0.12	1.9	2.1
0.7	85	15	2.8	2.0	0.6	2.6	0.78	0.22	2.6	2.9
0.75	72	28	4.3	2.5	1.7	4.2	0.62	0.38	4.1	4.5
0.8	63	37	8.0	4.0	4.0	8.0	0.52	0.48	7.7	8.5

$E$  is the alloy deposition potential (potential vs. standard hydrogen el.);  $j_{\Sigma}$ , summary current density during electrolysis;  $j_{Pb}$  and  $j_{Sn}$ , the partial current densities at lead and tin release to alloy (method of calculation is shown in our paper [18]);  $f_{Pb}$  and  $f_{Sn}$ , the fragments of surface on which lead and tin ion discharge takes place (method of calculation is shown in our paper [18]);  $j'_{Pb}$  and  $j'_{Sn}$ , are the partial current densities referred to the surface, on which lead and tin ion discharge to alloy takes place.

Fig. 4 shows that the relationship of such kind is well realized also in the case of the system under study (straight line in Fig. 4 is drawn with a slope ratio equal to 1, and the points are experimental data).

With reference to the system under study the following can be noted:

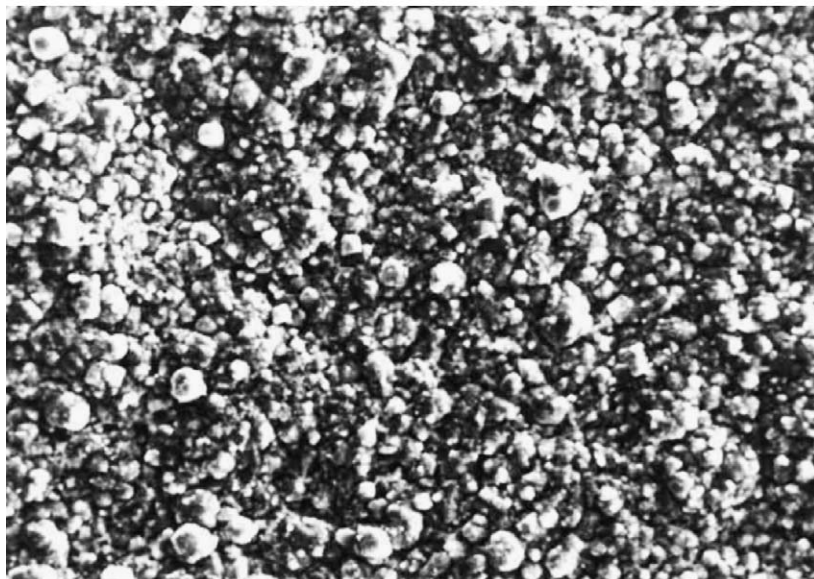
- absence of visible interaction between the alloy co-deposited components results in the fact that partial molar free energy of alloy formation in this case is equal to zero, and hence at deposition, both of tin in the alloy with tin and tin in alloy with lead no depolarization effects shall take place;

- among the factors, which can give rise to super-polarization effects, there can appear changes in zero charge potential at transition from pure metal deposition to deposition of the metal to alloy and this can change adsorption free energy of particle under reduction.

Fig. 5 makes it possible to evaluate change of zero charge potential,  $E_{z.ch.}$  at transition from tin to lead. Method of calculation of  $E_{z.ch.}$  is shown in [20]. According to Fig. 5, when lead content in the alloy exceeds 50%,  $E_{z.ch.}$  of the alloy is practically equal to  $E_{z.ch.}$  of lead, and hence at lead deposition on alloys Pb–Sn, alloyed with tin, the effects connected with change of conditions for adsorbing ions under discharge shall



(a)



(b)

Fig. 8. Microstructure of Pb–6 wt.% Sn–0.75 wt.% Zn alloy plating, obtained from hydrogen boron fluoride-electrolyte (a) and nitrilotriacetate-electrolyte (b). Magnification:  $\times 1000$ .



not take place. On the other side, tin ion discharge on alloys rich with lead shall run under super-polarization conditions, since  $E_{z.ch.}$  of alloy is more negative than  $E_{z.ch.}$  of tin.

Fig. 6 and Table 1 show that at low-current densities deposition of tin to alloy with lead actually runs at super-polarization, the value of which depending on current density (which is connected with considerable differences in angle factor values of partial polarization curve of tin deposition to alloy (curve 2, Fig. 6) and in pure form (curve 3, Fig. 6)), is within  $-0.2$  to  $0.03$  and on increasing,  $j_K^c$  the super-polarization effect disappears and is replaced by “depolarization”, the cause of which is the change of tin ions diffusion conditions (instead of the normal to the surface it is to a sphere in the form of separate tin grains in two-phase alloy).

Atomic absorption spectrometry and method inductive-coupled plasma (ICP) were used for investigation of alloys composition.

Study of electrolysis mode effect to quality and composition of plating has shown that increased current density (as the reduced temperature) results in reduced content of more positive metal–lead (in the alloy lead), and electrolyte stirring results in reduced content of more negative metal–tin (in the case of lead–tin alloy) or zinc (in the case of lead–tin–zinc alloy).

Effect of current density on structure of plating with double alloy lead–tin is shown in Fig. 7a and b. As current density increases, more coarse crystals are formed. Introduction of zinc into the double alloy tin–lead changes structure of the plating. Microstructure of plating with lead–tin alloy is shown in Fig. 7c and d represents microstructure of plating with lead–tin–zinc alloy, obtained at a current density of  $56 \text{ A m}^{-2}$ . Fig. 7 shows that plating of lead–tin–zinc alloy is more uniform and fine-crystalline. Fig. 7e and f shows how current density change the effects, the quality of plating, with lead–tin–zinc alloy. With current density increase, separate dendrites growth takes place.

Study of different SA effect on the quality of lead–tin and lead–tin–zinc alloys has shown that the PEG is an admixture, which exerts a considerable inhibiting action on the electroplating process. In the presence of PEG, dense fine-crystalline plating with good adhesion to the copper sheet has been obtained.

Porosity study (method is shown in [7]) has shown that the plating with alloy Pb–Sn–Zn, obtained from the NTA-electrolytes, has no pores even at a thickness of  $5 \mu\text{m}$ .

Based on the obtained results optimal composition of the NTA-electrolyte for applying underlayer of Pb–Sn–Zn alloy and electrolysis mode have been selected. Information about the method of ternary Pb–Sn–Zn alloys deposition is shown in [21]. Fragments of surface with Pb–Sn–Zn alloy plating obtained from the BFE-electrolyte and the NTA-electrolyte are shown in Fig. 8.

Study of corrosion resistance of lead plating with layer of lead–tin–zinc alloy has shown that the developed plating

has increased anti-corrosion characteristics as compared to plating of lead and tin and lead–tin alloy and can be used to protect ECMG of industrial batteries.

Storage batteries with negative electrodes, copper sheets of which have been protected by the proposed plating for the service life, have been tested. The tests have shown that the reliable protection ensures long service life and makes it possible to use copper in sealed storage batteries.

### 3. Conclusions

A new protective plating of ECMG in sealed storage batteries consisting of Pb–Sn–Zn corrosion-resistant layer and lead layer is represented.

The outlook of using nitrilotriacetate-electrolytes comprising SA for obtaining high-quality plating with lead, tin, lead–tin alloy and lead–tin–zinc alloys is shown.

Effect of the main technological parameters (concentration of components and solution pH, electrolyte stirring rate and temperature, current density) on the quality of the obtained plating is noted.

### References

- [1] N. Bagshow. Marine Storage Batteries, L. Sudostroenie, (Translation from English), 1986, p. 120.
- [2] S. Goodman, Batteries Int. 11 (1992) 105.
- [3] R. Kiessling, J. Power Sources 19 (2–3) (1987) 147–150.
- [4] N. Chunts, A. Rusin, M. Simonova, Studies in Sphere of Chemical Current Source Production Technology. Collected Book of NIAI Scientific Papers, L. Energoatomizdat, 1986, pp. 22–27.
- [5] Y. Kamenev, N. Chunts, E. Ostapenko, J. Power Sources 116 (2003) 169–173.
- [6] Author's Certificate No. 1391396 Russia, MKI5 H01M 4/68, 4/74, Electrode for Lead Storage Battery.
- [7] L.L. Shraier (Ed.), Corrosion: Reference Book, M.: Metallurgia, 1981, p. 736.
- [8] M. Dasoian, I. Aguf, Fundamentals of Lead Storage Battery Calculation, Design and Production Technology, L. Energia, 1978, p. 190.
- [9] Y. Kamenev, M. Lushina, A. Kiselevitch, A. Rusin, E. Ostapenko, J. Prikladnoy Khimii 74 (2) (2001) 220–225.
- [10] P. Viacheslavov, Alloy Electrolytic Depositing, L. Mashinostroenie, 1986, p. 112.
- [11] G. Kiriakov, V. Bryntseva, Zinc and Lead Corrosion in Sulfuric Solutions, Alma-Ata, Nauka, The Kazakh SSR, 1979, p. 72.
- [12] M. Shluger (Ed.), Electroplating in Machine Building, Reference Book, M. Mashinostroenie, vol. 1, 1985, p. 240 (in 2 volumes).
- [13] M. Lushina, G. Kolikova, J. Prikladnoy Khimii 67 (2) (1994) 296–299.
- [14] A. Tarelkin, V. Kravtsov, V. Kondratiev, Elektrokimiya 25 (7) (1989) 1000–1003.
- [15] A. Tarelkin. Equilibrium and Kinetics of Electrode Reactions of Lead Nitrilotriacetate Lead(II) and ZINC(II) Complexes. Author's Abstract of Ph.D. Thesis L, 1989, p. 16.

- [16] M. Lushina, B. Krasikov, J. Prikladnoy Khimii 64 (10) (1991) 2075–2078.
- [17] M. Lushina, B. Krasikov, J. Prikladnoy Khimii 67 (11) (1994) 1816–1819.
- [18] M. Lushina, B. Krasikov, J. Prikladnoy Khimii 68 (4) (1995) 558–562.
- [19] B. Krasikov, R. Astakhova, et al., J. Prikladnoy Khimii 45 (8) (1972) 1707–1713.
- [20] M. Grilihes, B. Krasikov, J. Prikladnoy Khimii 40 (4) (1967) 921–923.
- [21] Patent No. 2153739, Russia.